A Study on the Effects of Artifacts on Fatigue Limit of Ductile Cast Iron with Ferritic Structure

Jinhak Kim*
Department of Mechanical Engineering, Yeungnam University
Mingun Kim
Department of and Mechanical Engineering, Kangwon National University

In this study, fatigue tests were performed to examine the effects of micro drill hole on fatigue limit of as cast and austempered ductile cast iron (ADI) using the rotary bending fatigue tester. As results, micro drill holes (diameter$\leq 0.4mm$) did not influence the fatigue limit of ADI, compared to annealed ductile cast iron; the critical defect size of crack initiation, in ADI was larger than as cast. If the $\sqrt{area}s$ of micro drill hole and graphite nodule in ADI are comparable, crack initiates at the graphite nodule. When the ruggedness developes through austempering treatment process, microstructure on crack initiation at micro drill hole is tougher than that of as cast ductile cast iron.

Key Words : Fatigue, Fatigue Limit, Ferritic Structure, Micro Drill Hole, Graphite Nodule, Ductile Cast Iron, Austempering Treatment

1. Introduction

Ductile cast iron shows several engineering and manufacturing advantages over cast steels : damping capacity, wear resistance, manufacturing cost, and less volume shrinkage during solidification (Lampman, 1996). In particular, austempered is ductile cast iron(ADI) is an alloyed and heat treated ductile or nodular cast iron. It is considered as an important engineering material in recent years because of its excellent mechanical properties (Jenkins, 1990). ADI is used as structural components in wide diverse fields such as gears, crankshafts, locomotive wheels, agricultural equipments and so on. Due to its high strength with good ductility, good wear resistance, good fatigue properties and fracture toughness, ADI will find further engineering applications (Choi, 1990 ; Park, 1992).

We prepared ductile cast iron with ferritic structure (Fig. 1) for ADI. It then is subjected to an isothermal heat treatment process called austempering. Austempering process involves austenitizing the alloy in the temperature range of 870 to 980℃ for 1 to 2 hr and then quenching it to an intermediate temperature range of 260 to 500℃ and holding for 2 and 4 hr. This gives an unique microstructure in which the matrix consists of a mixture of ferrite and high carbon

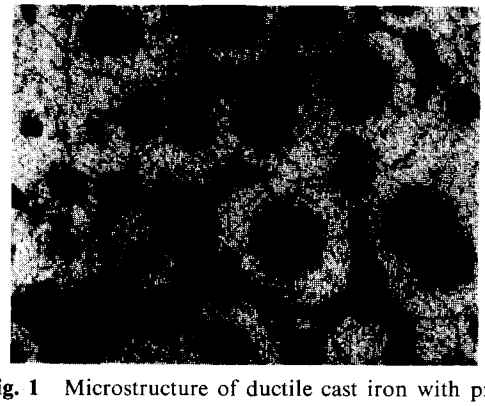

Fig. 1 Microstructure of ductile cast iron with predominantly ferritic structure, ×200

* Corresponding Author,
E-mail : crgreen@orgio.net
TEL : +82-61-450-6407 ; **FAX** : +82-61-452-6376
Department of Mechanical Engineering, Mokpo National University 61, Torim, Chonggye, Muan, Chonnam 534-729, Korea. (Manuscript **Received** September 22, 1999; **Revised** July 5, 2000)

austenite. This structure is often referred to as ausferrite (James, 1999). The microstructure also includes graphite nodules dispersed. The microstructure is different from austempered steels where the microstructure primarily consists of ferrite and carbide.

Most of studies on ADI have been done on ductile cast iron with pearlitic microstructure. Therefore, only limited information of the mechanical properties is available for ADI with ferritic as cast structure. Besides, the influence of defects on fatigue limit of ADI with ferritic as cast structure is not established yet.

The present study investigated the effects of artifacts or micro drill hole on the fatigue limit of the two ductile cast iron in indoor environment. We evaluated the fatigue crack origin through the $\sqrt{area}$ parameter which is an effective defect parameter to unify the geometry and size of diverse defects for high strength carbon steel (Murakami, 1993). The purpose of this work was to obtain the critical defect size governing the fatigue life of the two ductile cast irons for the actual application to diverse fields of industries.

2. Experimental Procedure

The material used for this study is a commercial grade products, GCD45 as per KS standard (KS D 4302, 1984). Chemical composition is listed in Table 1. Round cylindrical or plain specimens were prepared as per ASTM standard (ASTM, 1993) for rotary bending fatigue tester.

After fabrication, the plain samples were heat treated. As cast was stress relieved by heat treatment at 600℃ for 2 h, followed by cooling in air to room temperature. ADI was austenitized at 900℃ for 1 h, quenched into a salt bath and held 400℃ for 1 h, and then cooled in air to room temperature. During the austenitizing process, rapid specimens from furnace to the salt bath ensure that the austenite formed at high temperature would not transform to coarse pearlite.

Scanning electron microscope (SEM) photography of their structures are given in Fig. 2, after etching in 3% Nital. As cast structure is a typical bull's eye (predominantly ferrite and plus pearlite), and the ADI structure shows ausferrite (James, 1999) which is a mixture of acicular ferrite and austenite.

After heat treatment, the cylindrical or plain type specimens grounded and then polished with emery paper (grit level : from 80 to 2000) and allumina powder with 0.3 μm grit level to mirror surface, and then four kinds of artifacts or micro

Table 1 Chemical composition of experimental material (wt.%)

	C	Si	Mn	P	S	Mg	Fe
GCD45	3.75	3.0	0.15	0.03	0.015	0.04	Bal.

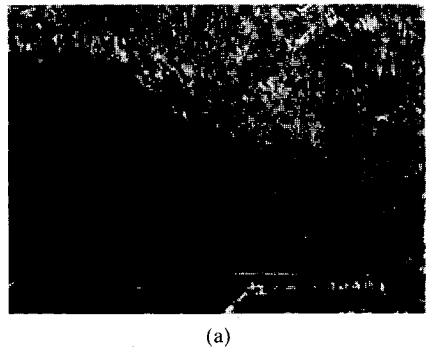

(a)

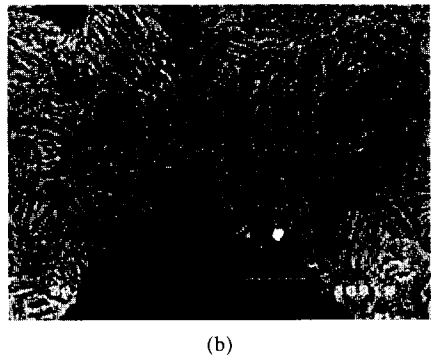

(b)

Fig. 2 Typical microstructures of two ductile cast iron, ×200, (a) As cast, (b) ADI

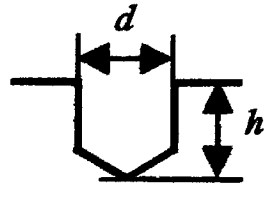

Fig. 3 Geometry of micro drill hole drilled on the center of minimum diameter, $d=h$

Table 2 Typical mechanical properties of the two ductile irons

	σ_Y	σ_B	δ	Hv
As cast	316	443	23.8	221
ADI	799	1065	9.4	512

σ_Y : Yield strength, 0.2% proof stress (MPa)
σ_B : Tensile strength (MPa)
δ : Elongation (%)
Hv : Vicker's hardness

Table 3 Characteristics of graphite nodule

	D_{sg}	H_{sg}	A_{sg}	N_{sg}
As cast	32	75	25	145
ADI	29	86	12	74

D_{sg} : Mean diameter (μm)
H_{sg} : Nodularity (%)
A_{sg} : Area fraction (%)
N_{sg} : Nodule count (count/mm^2)

drill holes, 0.1 mm, 0.2 mm, 0.3 mm and 0.4 mm ($d=h$) were machined on the center of minimum diameter of specimen using micro drilling machine before the tests. The geometry of micro drill hole is shown in Fig. 3. The depth of drill hole was regulated differently by 0.1 mm, to obtain the drill holes of diverse $\sqrt{area}$ values.

Mechanical property is measured for the two ductile cast irons and the data are given in Table 2. Five test samples were tested and the average was taken as the representative of the test data. Ultimate tensile strength, 0.2% offset yield strength and % elongation were obtained from the load against displacement plot. Micro vicker's hardness was averaged from 30 points with the indentation loads of 50 g on the samples. Also, Table 3 shows the characteristics of graphite nodule obtained by KS Standard (KS D 4302, 1984).

The average from three samples measurement was taken as the measurement data. Mean diameter, nodularity, area fraction and nodule count were also measured.

Tests were performed on a rotary bending fatigue tester ($R=-1.0$) at room air temperature, and on 60 Hz at 3500 rpm.

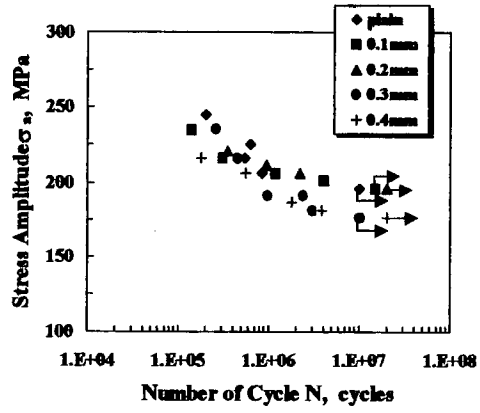

Fig. 4 S-N data of as cast

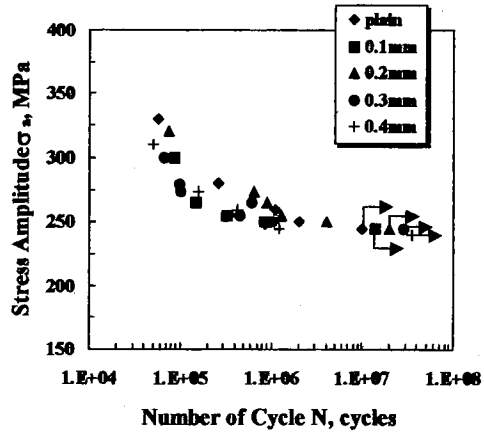

Fig. 5 S-N data of ADI

3. Results and Discussion

3.1 Effects of micro drill hole on fatigue limit

Rotary bending fatigue tests were run on plain and four kinds of micro drill holed specimens. The fatigue test results were shown in Figs. 4 and 5.

As shown in Fig. 4 with as cast, note that the micro drill holes of 0.1 mm~0.2 mm ($d=h$) did not reduce the fatigue limit while the limit decreased for 0.3 mm and 0.4 mm ($d=h$).

However, in Fig. 5 with ADI, the fatigue limit did not show a difference with plain specimen. We believe that the fatigue limit of ADI is not affected by the micro drill holes of 0.4 mm and below, due to the reinforced microstructure for-

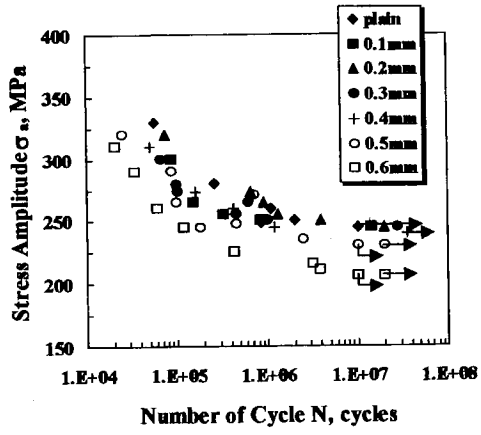

Fig. 6 S-N data of 0.5 *mm*, 0.6 *mm* micro drill hole in ADI

med during the austempering treatment process.

This observation conflicts with the prior study (Kato, 1997) that the fatigue strength of ADI conspicuously decrease due to the increment of defect sensitivity caused by austempering process to any artifacts.

Thus it is concluded from Fig. 5 that fatigue crack prefers to initiate at internal defect such as graphite nodule and casting defect rather than the micro drill holes.

To evaluate the artifacts sensitivity of fatigue limit, the tests were performed on the ADI specimen with 0.5 *mm* and 0.6 *mm* ($d=h$) micro drill holes, and presented in Fig. 6, along with Fig. 5. As in Fig. 6, the fatigue limits of the ADI specimen with 0.5 *mm* and 0.6 *mm* obviously decreased. We believe that the critical size of micro drill holes, being fatigue crack origin between as cast and ADI is different.

3.2 Estimation of the critical defect size for crack initiation with micro drill holes

Tables 5 and 6 present the estimation values of the $\sqrt{area}_c$ for fatigue crack initiation at micro drill hole, which are investigated with the as cast and ADI with micro drill holes under 1.1 times fatigue limit of plain specimen, $1.1\sigma_w$.

The depth (d) of micro drill hole was regulated differently by 0.1 *mm* using micro drilling machine (Self-manufactured, Range: 0.04~1 *mm*) with dial gage (Mitutoyo, Analysis capacity: 1 μm), to ensure that the micro drill hole has diverse $\sqrt{area}_{hole}$ value. The $\sqrt{area}_{hole}$ value was calculated by means of Eq. (1) (Murakami, 1983).

Table 4 Estimation of critical defect size in as cast specimen with different $\sqrt{area}_{hole}$

d (*mm*)	h (*mm*)	$area_{hole}$ (μm)	Origin	N_f (cycles)
0.30	0.20	217	hole	3.5×10^6
			defect	1.5×10^6
			defect	2.2×10^6
			defect	4.5×10^6
			defect	1.4×10^6
	0.30	278	hole	2.6×10^6
			defect	1.0×10^6
			defect	1.6×10^6
			defect	1.8×10^6
			defect	2.8×10^6
0.40	0.40	370	hole	5.5×10^5
			hole	6.2×10^5
			hole	5.9×10^5
			hole	4.8×10^5
			hole	5.1×10^5

$$\sqrt{area}_{hole}=\sqrt{hd-d^2/4\sqrt{3}} \quad (1)$$

where, h and d represent depth and diameter of micro drill hole as shown in Fig. 3. After fatigue test, SEM observation for the fatigue crack origin of as cast and ADI was carried out to clarify the fatigue crack origin.

It is observed from Table 4 that all fatigue cracks originate at micro drill holes in the case of $\sqrt{area}_{hole}$ 370 μm. Whereas in the case of 217 μm, most of fatigue cracks commence at the ruggedness of graphite nodule.

Based on the SEM observation of the fatigue crack origin in specimens with 278 μm of $\sqrt{area}_{hole}$, more than 50% the fatigue cracks were originated at micro drill hole.

For 370 μm and 278 μm together, the crack initiation at micro drill hole is about 80%. For

Table 5 Estimation of critical defect size in specimen with different $\sqrt{area}_{hole}$

d (mm)	h (mm)	$area_{hole}$ (μm)	Origin	N_f (cycles)
0.50	0.50	462	hole	1.3×10^6
			defect	2.3×10^6
			defect	1.8×10^6
			defect	3.5×10^6
			defect	2.9×10^6
0.60	0.50	495	hole	1.1×10^6
			hole	9.1×10^5
			defect	2.1×10^6
			hole	5.7×10^5
			defect	1.8×10^6
	0.60	555	hole	7.6×10^5
			hole	8.7×10^5
			hole	8.0×10^5
			hole	9.8×10^5
			hole	1.0×10^5

217 μm and 278 μm however, the rate is no more than 20%. On the other hand, from Table 5 in case of ADI, the 498 μm is about transitional.

The transition values are 278 μm to as cast and 498 μm to ADI, respectively. It was observed that when the $\sqrt{area}_{hole}$ is not less than 278 μm in as cast and not less than 498 μm in ADI, the fatigue crack initiation prefers micro drill holes to internal defect like graphite nodule. It therefore, supports the results of Fig. 4 and Fig. that the reduction of fatigue limit is observed in two ductile cast iron.

Because the $\sqrt{area}_{hole}$ value of 0.3 $mm(d=h)$ is equal to $\sqrt{area}_c$, the reduction of fatigue limit appears in the specimen with 0.3 mm micro drill hole in as cast. Meanwhile in ADI, $\sqrt{area}$ hole value of 0.4 $mm(d=h)$ was smaller than $\sqrt{area}_c$; thus the fatigue crack initiated at graphite nodule instead of the micro drill hole.

The fatigue crack origin in a fractured specimen with micro drill hole was observed by means of SEM. Table 6 presents the rates of graphite nodule and micro drill hole which are selected as fatigue crack origin in micro drill hole specimen. Focusing on the onset of fatigue crack at micro drill holes, crack initiation is merely 20% in the

Table 6 Rate of hole and defect being origin of fatigue crack

	Origin		Defect (%)
As cast	0.1 mm	20	80
	0.2 mm	20	80
	0.3 mm	83	17
	0.4 mm	100	0
ADI	0.1 mm	0	100
	0.2 mm	0	100
	0.3 mm	16	84
	0.4 mm	33	67

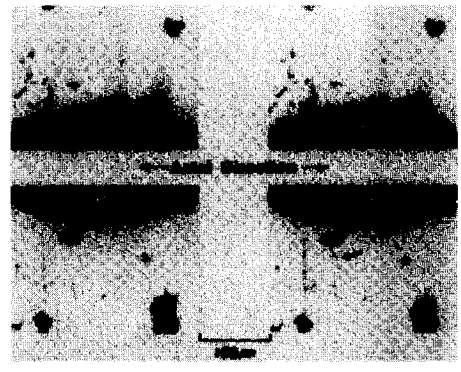

(a)

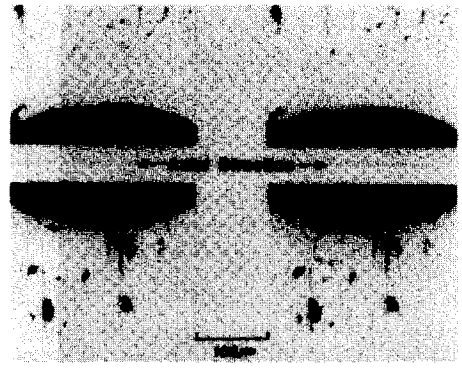

(b)

Fig. 7 Photography of onset of fatigue crack under 1.1 σ_w, arrow marks are crack length, (a) As cast, $N_i=1.5\times10^4$, (b) ADI, $N_i=7.2\times10^5$

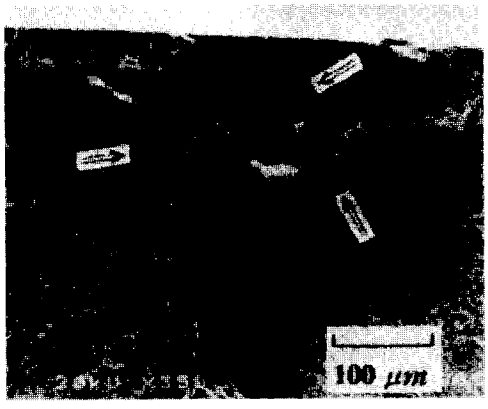

Fig. 8 Comparison of $\sqrt{area}$ of graphite and artificial defect in ADI, arrow marks are fatigue crack origin, $\sigma_a = 250$ MPa, $N_f = 6.1 \times 10^5$, $\sqrt{area}_{graphite} = 295\ \mu m$(graphite), $\sqrt{area}_{hole} = 278\ \mu m$(0.3 mm hole)

specimen with 0.1 $mm \sim 0.2\ mm(d=h)$ in as cast. While, in case of 0.3 $mm \sim 04\ mm$, the rate is about 80%. On the other hand, in ADI, that at the micro drill holes is less than 30% in most of specimens, and in the rests fatigue cracks commence at the graphite nodule.

It is therefore concluded that the estimated $\sqrt{area}_C$ can be a criterion to judge the fatigue crack initiation position.

Moreover, fatigue tests with the two ductile cast iron specimen with a micro hole ($d=h=0.6$ mm) under 1.1 σ_w investigated the initiation life of fatigue crack in first stage. Figure 7 shows the photography of the first stage fatigue crack.

As a results of the investigation, the first stage fatigue crack of about 80 μm length was observal at 1.5×10^4 cycles in as cast, and 7.2×10^5 cycles in ADI, respectively.

Therefore is that the lighen resistance to crack initiation at micro drill hole in ADI one of the reasons of low rate of crack initiation at micro drill hole. This supports the result of Fig. 5.

Figure 8 shows a SEM photograph that fatigue crack initiates at the edge of graphite nodule which exists just below the surface. And the fatigue crack is not affected by the micro drill hole of 0.3 $mm(d=h)$ on surface. The arrow marks show the fatigue crack origins. It from Fig. 8 that several fatigue cracks initiated at the ruggedness around graphite nodule, propagated and eventually led to fracture.

As a result of the investigation of $\sqrt{area}$ value of the graphite nodule by mesoscopic approximation (Kim and Kim, 1999), $\sqrt{area}_{graphite}$ was 295 μm which was al most same as that of 0.3 mm drill hole.

4. Conclusion

We investigated the effects of micro drill holes on fatigue limit in as cast and austempered ductile cast iron with rotary bending fatigue tests. We obtained follows results:

(1) Micro drill holes (diameter $\leq 0.4\ mm$) on specimen did not show the effects on fatigue limit in ADI as compared with annealed as cast ductile cast iron.

(2) The $\sqrt{area}_C$ (critical defect size to crack initiation at micro drill hole) of ADI is larger than that of as cast.

(3) The low rate of crack initiation at micro drill hole in ADI is due to the higher microstructure resistance to crack initiation at micro drill holes compared to as cast ductile cast iron.

(4) If the $\sqrt{area}s$ of micro drill hole and graphite nodules are eguivalent, crack at graphite nodule initiates prefera at micro drill hole. The serious ruggedness around graphite nodule was formed through austempering treatment process.

References

ASTM E 8M-86a, ASTM Standards, Philadelphia, PA, 03-01, 546, 1993. pp. 199~222.

Choi, D. C., 1990, "Widening Applications of Spheroidal Graphite Cast Iron," *The Jr. of the Korean Foundrymen's Society*, Vol. 10, No. 4, pp. 294~298.

Jenkins, L. R., Ductile Irons, 1990, *ASM Handbook*, Vol. 1, pp. 33~55.

James, M. N. and Wenfong, L., 1999, "Fatigue Crack Growth in Austempered and Grey Cast Irons-Stress Ratio Effects in Air and Mine Water," *Materials Science and Engineering*, A265, pp. 129~139.

KS D 4302, KS Standards, ROK, UDC 669.

131. 7, 1984, pp. 1~4.

Kato, Y. and Takafuji, S., 1997, "Fatigue Strength of Austempered Ductile Cast Iron in a Long Life Regime," *Transactions of the JSME*, Vol. 63, No. 610, pp. 1153~1158.

Kim, M. G. and Kim, J. H., 1999, "A Study on the Quantitative Evaluation of Defect Size Governing the Fatigue Reliability in Ductile Iron," *Proc. of the KSME 1999 Spring Annual Meeting A*, pp. 725~730.

Lampman, S. R., Fatigue and Fracture, 1996, *ASM Handbook*, Vol. 19, pp. 665~679.

Murakami, Y., 1993, Effects of Small Defects and Nonmetallic Inclusions, *Yokendo LTD.*, pp. 233~258.

Park, H. S. and Jin, D. K., 1993, "A Study on Corrosive Wear Characteristics and the Mechanism of Austempered Low-Alloy Ductile Iron," *Transactions of the KSME*, Vol. 17, No. 6, pp. 1404~1411.